Raman Study of Cooper Pairing Instabilities in $(Li_{1-x}Fe_x)OHFeSe$

G. He,[1,*] D. Li,[2,3] D. Jost,[1,4] A. Baum,[1] P. P. Shen,[2,3] X. L. Dong,[2,3,5] Z. X. Zhao,[2,3,5] and R. Hackl[1,4,†]

[1]*Walther Meissner Institut, Bayerische Akademie der Wissenschaften, 85748 Garching, Germany*
[2]*Beijing National Laboratory for Condensed Matter Physics, Institute of Physics, Chinese Academy of Sciences, Beijing 100190, China*
[3]*School of Physical Sciences, University of Chinese Academy of Sciences, Beijing 100049, China*
[4]*Fakultät für Physik E23, Technische Universität München, 85748 Garching, Germany*
[5]*Songshan Lake Materials Laboratory, Dongguan, Guangdong 523808, China*

(Received 20 June 2020; accepted 15 October 2020; published 17 November 2020)

We studied the electronic Raman spectra of $(Li_{1-x}Fe_x)OHFeSe$ as a function of light polarization and temperature. In the B_{1g} spectra alone we observe the redistribution of spectral weight expected for a superconductor and two well-resolved peaks below T_c. The nearly resolution-limited peak at 110 cm^{-1} (13.6 meV) is identified as a collective mode. The peak at 190 cm^{-1} (23.6 meV) is presumably another collective mode since the line is symmetric and its energy is significantly below the gap energy observed by single-particle spectroscopies. Given the experimental band structure of $(Li_{1-x}Fe_x)OHFeSe$, the most plausible explanations include conventional spin-fluctuation pairing between the electron bands and the incipient hole band and pairing between the hybridized electron bands. The absence of gap features in A_{1g} and B_{2g} symmetry favors the second case. Thus, in spite of various differences between the pnictides and chalcogenides, this Letter demonstrates the proximity of pairing states and the importance of band structure effects in the Fe-based compounds.

DOI: 10.1103/PhysRevLett.125.217002

The mechanism of Cooper pairing in Fe-based superconductors (FeSCs) or the copper-oxygen compounds is among the most vexing problems in condensed matter physics. The at least partial understanding of these unconventional superconductors would pave the way toward new materials. In either case, superconductivity occurs close to magnetic order [1]. Consequently, spin fluctuations are among the candidates for supporting electron pairing [2,3]. Alternatively, charge [4] or orbital fluctuations [5] between the Fe $3d$ orbitals, spin-orbit coupling [6], and/or nematic fluctuations [7] may support Cooper pairing. In all cases, the Fermi surface topology strongly influences the pairing tendencies and qualitative differences between the pnictides and chalcogenides may be expected and were scrutinized in doped $BaFe_2As_2$ (122) and FeSe-based (11) compounds.

Intercalated FeSe superconductors show T_c values higher than 40 K (Refs. [8,9]), but a Fermi surface topology different from the pnictides. In $(Li_{1-x}Fe_x)OHFeSe$, as shown in Fig. 1(a2), the holelike Fermi surface encircling the Γ point in 122 compounds and bulk FeSe cannot be resolved in angle-resolved photoemission spectroscopy (ARPES) any further [10] while it is still present in density functional theory [11], marking one of the similarities between intercalated and monolayer FeSe [10,12]. This similarity triggers the question as to the pairing interactions and the directly related gap structure. Neither the recent ARPES nor the tunneling experiments yielded clear answers here, but show only that there are essentially two rather different gap energies [13–15] on the presumably hybridized concentric electronlike Fermi surfaces [10].

Here electronic Raman scattering can contribute useful information [16–20]. In addition to the gap formation and the pair-breaking peaks at approximately twice the gap energy [21,22], collective excitations appear in the Raman

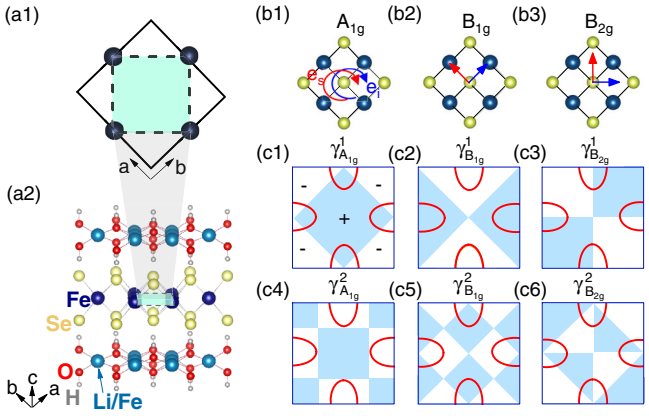

FIG. 1. (a1) 1 Fe (dashes) and 2 Fe (solid line) unit cells. (a2) The crystal structure of $(Li_{1-x}Fe_x)OHFeSe$. (b1)–(b3) Polarization configurations of A_{1g}, B_{1g}, and B_{2g} symmetries. The polarization configurations are indicated on the FeSe-layer. (c1)–(c3) First- and (c4)–(c6) second-order Raman vertices in the first Brillouin Zone (BZ, 1 Fe unit cell) of A_{1g}, B_{1g}, and B_{2g} symmetry, respectively, for the D_{4h} point group. The unfolded electron pockets are shown as red half ellipses.

response, which are related to details of the pairing potential $V_{\mathbf{k}\mathbf{k}'}$. Collective excitations in superconductors were first discussed by Bardasis and Schrieffer (BS) [23] and by Leggett [24]. The BS mode stems from a subleading pairing interaction that is orthogonal to the ground state. The Leggett mode is best thought of as interband Josephson-like number-phase fluctuation, the absolute energy of which corresponds to the relative coupling strength between the bands in comparison to the intraband coupling [25,26]. Thus, the careful study of putative collective modes offers an opportunity to clarify the competing superconducting instabilities and the related pairing glue.

In this Letter, we present polarization-dependent Raman spectra for temperatures between 7.2 and 48 K in high-quality single-crystalline $(Li_{1-x}Fe_x)$OHFeSe thin films with $T_c = 42$ K. At 7.2 K we observe two well-defined features at 110 and 190 cm^{-1} in B_{1g} but not in A_{1g} and B_{2g} symmetry. We conclude that at least the resolution-limited line at 110 cm^{-1} is a collective mode being either related to a subleading pairing interaction or a number-phase oscillation between the electron bands. The superconducting ground state in $(Li_{1-x}Fe_x)$OHFeSe may result from either spin fluctuations between the electron bands and the incipient hole band or the interaction between the hybridized electron bands.

$(Li_{1-x}Fe_x)$OHFeSe ($x \sim 0.18$) thin films were grown epitaxially on $(00l)$-oriented $LaAlO_3$ substrates as reported previously [27,28]. The thin films have a typical thickness of 100 nm and were characterized by x-ray diffraction and magnetization measurements showing a high crystallinity and a superconducting transition at $T_c = 42 \pm 1$ K (see Supplemental Material [29]). The Raman experiments were carried out with a standard light scattering equipment [16]. For excitation we used a solid-state and an Ar^+ laser emitting at 577 and 457 nm, respectively. All spectra were measured with an absorbed laser power of $P_{\mathrm{abs}} = 2$ mW limiting the heating in the spot to below 1.5 K/mW (see Supplemental Material [29]). The polarizations of the incoming and scattered photons will be defined with respect to the 1 Fe unit cell as shown in Figs. 1(b1)–1(b3), which are more appropriate for electronic excitations. We show Raman susceptibilities $R\chi''(T,\Omega) = S(\Omega,T)\{1 + n(T,\Omega)\}^{-1}$, where R is an experimental constant, $S(\Omega,T)$ is the dynamical structure factor that is proportional to the rate of scattered photons, and $n(T,\Omega)$ is the Bose-Einstein distribution function. The first- and second-order crystal harmonics of each symmetry which Raman vertices are proportional to and the position of the Fermi pockets of $(Li_{1-x}Fe_x)$OHFeSe are shown in Figs. 1(c1)–1(c6) to illustrate the relation between electronic Raman response in different symmetries and the Fermi surface topology.

Figure 2 shows the polarization-dependent Raman response of $(Li_{1-x}Fe_x)$OHFeSe above (red) and below (blue) T_c. The peaks observed at approximately 167 cm^{-1} in A_{1g} symmetry [Fig. 2(e)] and 205 cm^{-1} in B_{2g} symmetry [Fig. 2(c)] correspond to Se in-phase and Fe out-of-phase vibrations along the c axis, respectively [34]. The peak at 165 cm^{-1} in the B_{1g} spectra [Fig. 2(a)] can be identified as a leakage from the A_{1g} phonon. The small line width and high intensity of the phonon lines underpin the excellent crystalline quality of the sample. Because of surface contamination, broad peaks at 240 cm^{-1} [Fig. 2(a)], 224 and 256 cm^{-1} [Fig. 2(c)], and 252 cm^{-1} [Fig. 2(e)] in B_{1g}, B_{2g}, and A_{1g} symmetry, respectively, appear in the spectra. These peaks probably originate from Fe oxide phonons since they disappear after cleaving and are discussed in more detail in Supplemental Material [29].

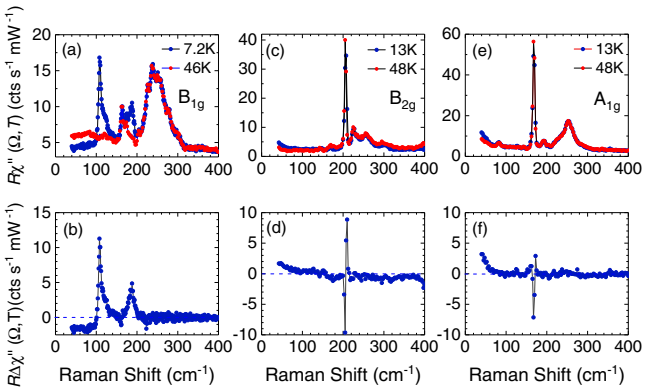

FIG. 2. (a),(c),(e) Raman spectra of $(Li_{1-x}Fe_x)$OHFeSe in B_{1g}, B_{2g}, and A_{1g} symmetry. (b),(d),(f) Difference spectra between superconducting and normal state.

If the normal state spectra are subtracted from the superconducting spectra, all phonons and extra lines disappear since they do not change appreciably upon crossing T_c as shown in Figs. 2(b), 2(d), and 2(f). However, due to the high spectral resolution, even small changes of the phonon lines can be identified.

The small changes in the phonon lines are the only detectable effects of superconductivity in A_{1g} and B_{2g} symmetry. The increase toward zero energy is an artifact resulting from insufficient rejection of the laser line. The spectral changes in B_{1g} symmetry are resolved clearly since the extra peaks at approximately 110 and 190 cm^{-1} have an intensity comparable to that of the phonons. In addition to the peaks, the continuum is suppressed below 90 cm^{-1} and is nearly energy independent. None of the excitations display appreciable resonance behavior, and the data can be reproduced in different regions of the sample, as shown in Supplemental Material [29]. The suppression and the additional peaks indicate a relation to superconductivity.

The most important observations include the following:

(i) There is no intensity redistribution below T_c in A_{1g} and B_{2g} symmetry, as observed earlier [19,35]. The phenomenon can be understood qualitatively in terms of the related polarization-dependent Raman form factors, the

TABLE I. Comparison between the peak positions in the B_{1g} Raman spectra and the gap energies obtained by STS and ARPES.

	Raman (cm^{-1})	Raman (meV)		STS (meV) [13,15]	ARPES (meV) [10]
$\Omega^{(1)}_{peak}$	110 ± 0.5	13.75 ± 0.06	$2\Delta_1$	17.2 ± 2.0	...
$\Omega^{(2)}_{peak}$	190 ± 0.5	23.75 ± 0.06	$2\Delta_2$	28.4 ± 4.0	26.0 ± 4.0
$\Omega^{(1)}_{peak}/k_BT_c$	3.80 ± 0.02		$2\Delta_1/k_BT_c$	4.75 ± 0.55	...
$\Omega^{(2)}_{peak}/k_BT_c$	6.56 ± 0.02		$2\Delta_2/k_BT_c$	7.84 ± 1.10	7.18 ± 1.10

Fermi surface topology of $(Li_{1-x}Fe_x)$OHFeSe as shown in Figs. 1(c1) and 1(c3), and screening effects.

(ii) The B_{1g} spectrum is suppressed below 90 cm^{-1}. This indicates a nearly isotropic superconducting gap, as already observed for $Rb_{0.8}Fe_{1.6}Se_2$ [19]. The residual intensity of approximately 2–3 counts $(s\,mW)^{-1}$ is not entirely clear but may either originate from the substrate, surface layers, or luminescence. In agreement with the scanning tunneling spectroscopy (STS) results [13], there is no reason to assume that there are states inside the gap. Similar residual Raman intensities are also observed in single crystals of pnictides and other chalcogenides [19,20,36] and can safely be assumed to be extrinsic.

(iii) There are two superconductivity-induced features separated by some 80 cm^{-1}. Gap features at a similar separation but slightly higher energies were observed by STS and ARPES as summarized in Table I. The significant differences in the derived gap energies presumably have a real physical reason, such as a substantial energy difference between the gap and collective modes [37]. The line at 190 cm^{-1} is nearly symmetric and 10–12 cm^{-1} wide, while that at 110 cm^{-1} is rather sharp around the maximum but asymmetric.

(iv) The peak at 110 cm^{-1} is nearly resolution-limited. For its width, it cannot result from pair breaking alone. Rather the symmetric line at 110 cm^{-1} having a FWHM of less than 5 cm^{-1} is a collective mode, while the shoulder on the high-energy side originates from pair breaking. We will explore this possibility later by a phenomenological analysis.

In Fig. 3, we show the variation with temperature of the B_{1g} difference spectra. With increasing temperature, the two peaks shift to lower energy and cannot be resolved any further above 38 K. Both peaks depend more weakly on temperature than expected from the BCS theory. As opposed to the results in $Ba_{1-x}K_xFe_2As_2$ [20], this temperature dependence does not allow us to clearly identify the origin of the superconducting structures. Whereas the pair-breaking peaks do not necessarily follow the BCS prediction, except in weakly interacting systems [38], at least BS collective modes are expected to follow the related single-particle gap $\Delta(T)$ [39]. The temperature dependence of Leggett modes has not been analyzed yet, but is presumably more complicated since the coupling of at least two gaps has to be considered [40,41]. Thus, the variation with temperature is not an identification criterion.

What are the possible explanations and the implications thereof for superconductivity in $(Li_{1-x}Fe_x)$OHFeSe? Given the STS and ARPES results, a scenario with two isotropic s-wave gaps appears to be natural and compatible with the Raman spectra. However, the gap energies observed by Raman scattering are significantly too small (Table I), and the phenomenology returns poor agreement with the data (see Supplemental Material [29]). Rather, the shape of the line at 110 cm^{-1} is strongly indicative of a collective mode. An undamped quadrupolar excitation inside the gap [42] or a nematic resonance [43,44] is not very likely since the

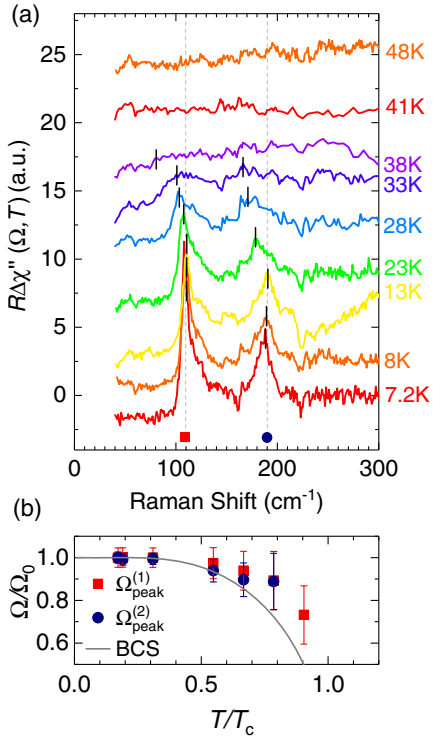

FIG. 3. (a) Temperature dependence of the difference spectra in B_{1g} symmetry. For clarity, data other than those measured at the lowest temperature are shifted vertically. The peak positions are marked by the black vertical lines. Two dashed lines indicate the peak positions at 7.2 K. The increase of the 13 K spectrum toward higher energies originates from a local surface contamination. (b) Normalized temperature dependence of peak positions. They are extracted by a fit with a Lorentzian function. For normalization of the energy, the $\Omega_0 = 110$ and 190 cm^{-1} for peak 1 and peak 2, respectively.

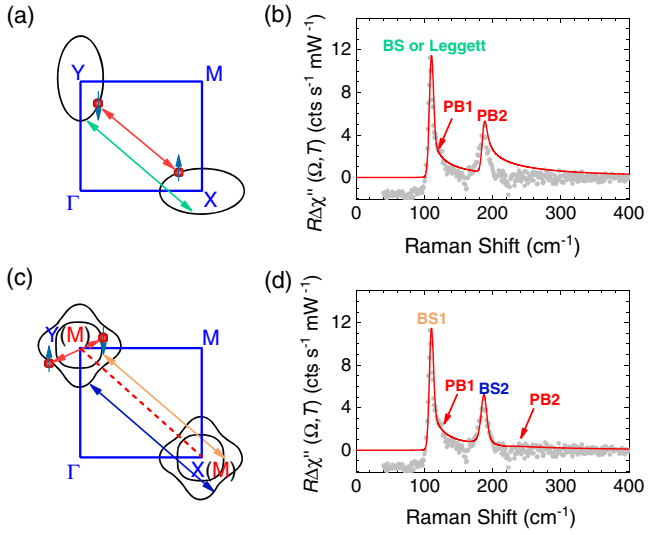

FIG. 4. Interactions and related phenomenological spectra. (a), (c) Illustration of the superconducting ground state and possible subdominant interactions in the first BZ. The blue solid lines indicate the first quadrant of the 1 Fe BZ boundary in (a) and (c). The 2 Fe BZ boundary in (c) is illustrated by the red dashed line. The Fermi pockets are shown by the black solid curves. The red double arrows indicate the pairing interaction in (a) and (c). The green double arrow in (a) and the orange and dark blue ones in (c) indicate the possible subdominant pairing interactions. (b),(d) The fitting results correspond to the situations in (a) and (c). The red curves are the fitting results. The gray solid dots are the experimental data. The BS modes or Leggett mode and pair-breaking (PB) peaks are indicated in (b) and (d).

related fluctuations above T_c could not be observed (see Supplemental Material [29]). The distinction between a BS and a Leggett mode is less obvious. Since the mode is apparently below the edge of the smaller gap, the damping is small in either case.

A BS mode indicates orthogonal pairing channels [23]. Given the possible interactions between the two electron bands at the X and Y points, as shown in Fig. 4(a), only a $d_{x^2-y^2}$ gap of lowest (first) order is possible if spin fluctuations are relevant. In this case the gaps on the two bands have opposite sign and, since there are no nodes on the Fermi surface, the gap is clean in agreement with the STS and Raman results. Then the BS mode would result from a $d_{x^2-y^2}$ interaction of second or higher order [for second-order B_{1g} symmetry, cf. Fig. 1(c5)], having a smaller coupling strength than the ground state. The description of the asymmetric maximum at 110 cm^{-1} is reasonable, as shown in Fig. 4(b), and yields a coupling strength of approximately 0.16 for the subleading channel (see Supplemental Material [29]).

This interpretation favors pair breaking as a possible explanation for the high-energy peak at 190 cm^{-1}. However, the symmetric shape is untypical for a pair-breaking feature and may only be explained by a broader gap distribution, as suggested by the STS data, for instance (see Table I). Yet, the energy of 190 cm^{-1} (23.6 meV) is significantly below the single-particle gap. More importantly, it is difficult to explain why there should be two rather distinct gaps for this scenario of equivalent bands. It is, in fact, more likely that there is a (π,π) reconstruction of the Fermi surface and a hybridization between the electron bands, as suggested by Khodas *et al.* [41,45]. Then one expects two concentric Fermi surfaces with distinctly different gaps, as seen here in the Raman data and also in the STS data [13,15]. ARPES [10] and STS [13] tell us that the outer Fermi surface has the larger gap. Superconductivity would then arise from the comparably strong interaction between these hybridized bands, inducing a repulsion of the gap energies [14] and either a collective Leggett mode in the A_{1g} channel [46] or a double-peak structure well below the gap for certain parameter ranges in the case of a sign change of the gap between the bands ($s_\pm$ gap) [45].

Since only the B_{1g} channel displays a distinct redistribution of spectral weight, below T_c scenarios that include other channels are less likely to explain the results. Thus, in addition to the strongly coupled ground state resulting from the interaction between the concentric bands, there must be a weaker (π,π) interaction leading to collective modes in B_{1g} symmetry, as shown in Fig. 4(c). In this scenario, the sharp mode is either a Leggett mode from a weak (π,π) coupling between X and Y on top of the strongly coupled ground state resulting from the strong coupling of the concentric bands or a BS mode having a similar origin. Huang *et al.* [47] indeed argue that the distinction between Leggett and BS modes becomes obsolete here.

The only remaining issue concerns the positions of the Raman peaks that appear at smaller energies than in the single-particle spectroscopies. Whereas the energy of the Raman maximum at 110 cm^{-1} is naturally explained in terms of a BS mode appearing below the related single-particle gap at 136 cm^{-1} (17 meV) and manifesting itself as a shoulder in the Raman spectrum, the position of the mode at 190 cm^{-1} is less obvious since there is no additional pair-breaking feature in the spectra. In principle, it could be another BS mode pulled down by 10% from the gap edge at approximately 220 cm^{-1} (27 meV) and suppressing the pair breaking almost entirely. Also in this case the ground state would be induced by a strong hybridization of the two electron bands. The resulting description of the experimental data is in fact much better in this case [see Fig. 4(d)].

Finally, since the hole band is rather close to the Fermi surface, spin-fluctuation pairing between the incipient hole band and the electron bands can still be rather strong [48,49]. Then the ground state is $s_\pm$ with all the electron bands having the same sign, and the B_{1g} modes are collective d-wave modes from the hybridized electron bands. Whether or not the magnitudes of the gaps observed on the electron bands and the related subleading pairing strengths are compatible with these considerations needs to

be worked out theoretically. The resulting spectra could be very similar to those in the previous case. However, due to the pairing-induced renormalization of the central hole band below T_c, one would not expect the A_{1g} spectra to be entirely insensitive to superconductivity. Thus, the scenario of an incipient band is less supported by the present experiment.

In conclusion, we studied the polarization- and temperature-dependent Raman spectra in $(Li_{1-x}Fe_x)$OHFeSe. Superconductivity affects only the B_{1g} spectra. One of the observed modes is resolution limited, arguing strongly for its collective character. For the surprisingly successful description of the data in terms of BS modes there are essentially two scenarios: (i) dominant pairing between the hybridized electron bands [41] and subleading (π, π) interactions between the electron bands. Then Leggett and BS modes cannot be distinguished [47]. (ii) If the ground state originates from the interaction between the incipient hole band and the electron bands, a similar collective mode may be expected, but completely inert A_{1g} spectra are unlikely in this case, making scenario (i) more likely. Yet, the distinction between the two scenarios requires quantitative theoretical studies.

We thank L. Benfatto, P. Hirschfeld, T. Maier, and L. Zhao for fruitful discussions. This work is supported by the Deutsche Forschungsgemeinschaft (DFG) through the coordinated programme TRR80 (Projekt-ID 107745057) and project HA2071/12-1. G. H. would like to thank the Alexander von Humboldt Foundation for support from a research fellowship. The work at China was supported by National Natural Science Foundation of China (No. 11834016), and the National Key Research and Development Program of China (Grant No. 2017YFA0303003) and Key Research Program of Frontier Sciences of the Chinese Academy of Sciences (Grant No. QYZDY-SSW-SLH001).

*Corresponding author.
Ge.He@wmi.badw.de
†Corresponding author.
Hackl@wmi.badw.de

[1] J. Paglione and R. L. Greene, High-temperature superconductivity in iron-based materials, Nat. Phys. **6**, 645 (2010).
[2] I. I. Mazin, D. J. Singh, M. D. Johannes, and M. H. Du, Unconventional Superconductivity with a Sign Reversal in the Order Parameter of $LaFeAsO_{1-x}F_x$, Phys. Rev. Lett. **101**, 057003 (2008).
[3] D. J. Scalapino, A common thread: The pairing interaction for unconventional superconductors, Rev. Mod. Phys. **84**, 1383 (2012).
[4] S. Onari and H. Kontani, Violation of Anderson's Theorem for the Sign-Reversing s-Wave State of Iron-Pnictide Superconductors, Phys. Rev. Lett. **103**, 177001 (2009).
[5] H. Kontani and S. Onari, Orbital-Fluctuation-Mediated Superconductivity in Iron Pnictides: Analysis of the Five-Orbital Hubbard-Holstein Model, Phys. Rev. Lett. **104**, 157001 (2010).
[6] S. V. Borisenko, D. V. Evtushinsky, Z. H. Liu, I. Morozov, R. Kappenberger, S. Wurmehl, B. Büchner, A. N. Yaresko, T. K. Kim, M. Hoesch, T. Wolf, and N. D. Zhigadlo, Direct observation of spin–orbit coupling in iron-based superconductors, Nat. Phys. **12**, 311 (2016).
[7] S. Lederer, Y. Schattner, E. Berg, and S. A. Kivelson, Enhancement of Superconductivity near a Nematic Quantum Critical Point, Phys. Rev. Lett. **114**, 097001 (2015).
[8] X. F. Lu *et al.*, Coexistence of superconductivity and antiferromagnetism in $(Li_{0.8}Fe_{0.2})$OHFeSe, Nat. Mater. **14**, 325 (2015).
[9] M. Burrard-Lucas, D. G. Free, S. J. Sedlmaier, J. D. Wright, S. J. Cassidy, Y. Hara, A. J. Corkett, T. Lancaster, P. J. Baker, S. J. Blundell, and S. J. Clarke, Enhancement of the superconducting transition temperature of FeSe by intercalation of a molecular spacer layer, Nat. Mater. **12**, 15 (2013).
[10] L. Zhao *et al.*, Common electronic origin of superconductivity in (Li,Fe)OHFeSe bulk superconductor and single-layer $FeSe/SrTiO_3$ films, Nat. Commun. **7**, 10608 (2016).
[11] I. A. Nekrasov and M. V. Sadovskii, Electronic and magnetic properties of the new iron-based superconductor $[Li_{1-x}Fe_xOH]FeSe$, JETP Lett. **101**, 47 (2015).
[12] X. Shi, Z.-Q. Han, X.-L. Peng, P. Richard, T. Qian, X.-X. Wu, M.-W. Qiu, S. C. Wang, J. P. Hu, Y.-J. Sun, and H. Ding, Enhanced superconductivity accompanying a Lifshitz transition in electron-doped FeSe monolayer, Nat. Commun. **8**, 14988 (2017).
[13] Z. Y. Du, X. Yang, H. Lin, D. L. Fang, G. Du, J. Xing, H. Yang, X. Y. Zhu, and H. H. Wen, Scrutinizing the double superconducting gaps and strong coupling pairing in $(Li_{1-x}Fe_x)$OHFeSe, Nat. Commun. **7**, 10565 (2016).
[14] Z. Y. Du, X. Yang, D. Altenfeld, Q. Q. Gu, H. Yang, I. Eremin, P. J. Hirschfeld, I. I. Mazin, H. Lin, X. Y. Zhu, and H. H. Wen, Sign reversal of the order parameter in $(Li_{1-x}Fe_x)OHFe_{1-y}Zn_ySe$, Nat. Phys. **14**, 134 (2018).
[15] C. Chen, Q. Liu, T. Z. Zhang, D. Li, P. P. Shen, X. L. Dong, Z. X. Zhao, T. Zhang, and D. L. Feng, Quantized conductance of Majorana zero mode in the vortex of the topological superconductor $(Li_{0.84}Fe_{0.16})$OHFeSe, Chin. Rev. Lett. **36**, 057403 (2019).
[16] T. P. Devereaux and R. Hackl, Inelastic light scattering from correlated electrons, Rev. Mod. Phys. **79**, 175 (2007).
[17] D. J. Scalapino and T. P. Devereaux, Collective *d*-wave exciton modes in the calculated Raman spectrum of Fe-based superconductors, Phys. Rev. B **80**, 140512(R) (2009).
[18] S. Maiti, T. A. Maier, T. Böhm, R. Hackl, and P. J. Hirschfeld, Probing the Pairing Interaction and Multiple Bardasis-Schrieffer Modes Using Raman Spectroscopy, Phys. Rev. Lett. **117**, 257001 (2016).
[19] F. Kretzschmar, B. Muschler, T. Böhm, A. Baum, R. Hackl, H. H. Wen, V. Tsurkan, J. Deisenhofer, and A. Loidl, Raman-Scattering Detection of Nearly Degenerate *s*-Wave and *d*-Wave Pairing Channels in Iron-Based $Ba_{0.6}K_{0.4}Fe_2As_2$ and $Rb_{0.8}Fe_{1.6}Se_2$ Superconductors, Phys. Rev. Lett. **110**, 187002 (2013).
[20] T. Böhm, A. F. Kemper, B. Moritz, F. Kretzschmar, B. Muschler, H. M. Eiter, R. Hackl, T. P. Devereaux,

D. J. Scalapino, and H. H. Wen, Balancing Act: Evidence for a Strong Subdominant d-Wave Pairing Channel in $Ba_{0.6}K_{0.4}Fe_2As_2$, Phys. Rev. X **4**, 041046 (2014).

[21] A. A. Abrikosov and L. A. Fal'kovskii, Raman scattering of light in superconductors, Zh. Eksp. Teor. Fiz. **40**, 262 (1961) [Sov. Phys. JETP **13**, 179 (1961), http://www.jetp.ac.ru/cgi-bin/e/index/e/13/1/p179?a=list].

[22] M. V. Klein and S. B. Dierker, Theory of Raman scattering in superconductors, Phys. Rev. B **29**, 4976 (1984).

[23] A. Bardasis and J. R. Schrieffer, Excitons and plasmons in superconductors, Phys. Rev. **121**, 1050 (1961).

[24] A. J. Leggett, Number-phase fluctuations in two-band superconductors, Prog. Theor. Phys. **36**, 901 (1966).

[25] M. V. Klein, Theory of Raman scattering from Leggett's collective mode in a multiband superconductor: Application to MgB_2, Phys. Rev. B **82**, 014507 (2010).

[26] G. Blumberg, A. Mialitsin, B. S. Dennis, M. V. Klein, N. D. Zhigadlo, and J. Karpinski, Observation of Leggett's Collective Mode in a Multiband MgB_2 Superconductor, Phys. Rev. Lett. **99**, 227002 (2007).

[27] Y. L. Huang, Z. P. Feng, S. L. Ni, J. Li, W. Hu, S. B. Liu, Y. Y. Mao, H. X. Zhou, F. Zhou, K. Jin, H. B. Wang, J. Yuan, X. L. Dong, and Z. X. Zhao, Superconducting (Li,Fe)OHFeSe film of high quality and high critical parameters, Chin. Rev. Lett. **34**, 077404 (2017).

[28] Y. L. Huang, Z. P. Feng, J. Yuan, W. Hu, J. Li, S. L. Ni, S. B. Liu, Y. Y. Mao, H. X. Zhou, H. B. Wang, F. Zhou, G. M. Zhang, K. Jin, X. L. Dong, and Z. X. Zhao, Matrix-assisted fabrication and exotic charge mobility of (Li,Fe)OHFeSe superconductor films, arXiv:1711.02920.

[29] See Supplemental Material at http://link.aps.org/supplemental/10.1103/PhysRevLett.125.217002 for sample characterization, determination of the spot temperature, surface quality, resonances, data reproducibility, phenomenology of collective modes, and fluctuations, which includes Refs. [30–33].

[30] S. H. Shim and T. S. Duffy, Raman spectroscopy of Fe_2O_3 to 62 GPa, Am. Mineral. **87**, 318 (2002).

[31] V. G. Sathe and A. Dubey, Broken symmetry in $LaAlO_3$ single crystal probed by resonant Raman spectroscopy, J. Phys. Condens. Matter **19**, 382201 (2007).

[32] F. Kretzschmar, T. Böhm, U. Karahasanović, B. Muschler, A. Baum, D. Jost, J. Schmalian, S. Caprara, M. Grilli, C. Di Castro, J. G. Analytis, J. H. Chu, I. R. Fisher, and R. Hackl, Critical spin fluctuations and the origin of nematic order in $Ba(Fe_{1-x}Co_x)_2As_2$, Nat. Phys. **12**, 560 (2016).

[33] S. Lederer, D. Jost, T. Böhm, R. Hackl, E. Berg, and S. A. Kivelson, Measuring the imaginary-time dynamics of quantum materials, Philos. Mag. **100**, 2477 (2020).

[34] A. Zhang, X. Ma, Y. Wang, S. Sun, B. Lei, H. Lei, X. Chen, X. Wang, C. Chen, and Q. Zhang, Probing the direct factor for superconductivity in FeSe-Based Superconductors by Raman Scattering, Phys. Rev. B **100**, 060504(R) (2019).

[35] B. Muschler, W. Prestel, R. Hackl, T. P. Devereaux, J. G. Analytis, J. H. Chu, and I. R. Fisher, Band- and momentum-dependent electron dynamics in superconducting $Ba(Fe_{1-x}Co_x)_2As_2$ as seen via electronic Raman scattering, Phys. Rev. B **80**, 180510(R) (2009).

[36] D. Jost, J.-R. Scholz, U. Zweck, W. R. Meier, A. E. Böhmer, P. C. Canfield, N. Lazarević, and R. Hackl, Indication of subdominant *d*-wave interaction in superconducting $CaKFe_4As_4$, Phys. Rev. B **98**, 020504(R) (2018).

[37] T. Böhm, F. Kretzschmar, A. Baum, M. Rehm, D. Jost, R. H. Ahangharnejhad, R. Thomale, C. Platt, T. A. Maier, W. Hanke, B. Moritz, T. P. Devereaux, D. J. Scalapino, S. Maiti, P. J. Hirschfeld, P. Adelmann, T. Wolf, H. H. Wen, and R. Hackl, Microscopic origin of Cooper pairing in the iron-based superconductor $Ba_{1-x}K_xFe_2As_2$, npj Quantum Mater. **3**, 48 (2018).

[38] T. P. Devereaux and D. Einzel, Electronic Raman scattering in superconductors as a probe of anisotropic electron pairing, Phys. Rev. B **51**, 16336 (1995).

[39] H. Monien and A. Zawadowski, Theory of Raman scattering with final-state interaction in high-T_c BCS superconductors: Collective modes, Phys. Rev. B **41**, 8798 (1990).

[40] H. Suhl, B. T. Matthias, and L. R. Walker, Bardeen-Cooper-Schrieffer Theory of Superconductivity in the Case of Overlapping Bands, Phys. Rev. Lett. **3**, 552 (1959).

[41] M. Khodas and A. V. Chubukov, Interpocket Pairing and Gap Symmetry in Fe-Based Superconductors with Only Electron Pockets, Phys. Rev. Lett. **108**, 247003 (2012).

[42] V. K. Thorsmølle, M. Khodas, Z. P. Yin, C. L. Zhang, S. V. Carr, P. C. Dai, and G. Blumberg, Critical quadrupole fluctuations and collective modes in iron pnictide superconductors, Phys. Rev. B **93**, 054515 (2016).

[43] Y. Gallais, I. Paul, L. Chauvière, and J. Schmalian, Nematic Resonance in the Raman Response of Iron-Based Superconductors, Phys. Rev. Lett. **116**, 017001 (2016).

[44] J. Kang and R. M. Fernandes, Superconductivity in FeSe Thin Films Driven by the Interplay between Nematic Fluctuations and Spin-Orbit Coupling, Phys. Rev. Lett. **117**, 217003 (2016).

[45] M. Khodas, A. V. Chubukov, and G. Blumberg, Collective modes in multiband superconductors: Raman scattering in iron selenides, Phys. Rev. B **89**, 245134 (2014).

[46] T. Cea and L. Benfatto, Signature of the Leggett mode in the A_{1g} Raman response: From MgB_2 to iron-based superconductors, Phys. Rev. B **94**, 064512 (2016).

[47] W. Huang, M. Sigrist, and Z. Y. Weng, Identifying the dominant pairing interaction in high-T_c FeSe superconductors through Leggett modes, Phys. Rev. B **97**, 144507 (2018).

[48] A. Linscheid, S. Maiti, Y. Wang, S. Johnston, and P. J. Hirschfeld, High T_c via Spin Fluctuations from Incipient Bands: Application to Monolayers and Intercalates of FeSe, Phys. Rev. Lett. **117**, 077003 (2016).

[49] V. Mishra, D. J. Scalapino, and T. A. Maier, $s_\pm$ pairing near a Lifshitz transition, Sci. Rep. **6**, 32078 (2016).